Fraction of a Millimeter Propagation of Exciton Polaritons in Photoexcited Nanofibers of Organic Dye

Ken Takazawa,[*] Jun-ichi Inoue, Kazutaka Mitsuishi, and Tadashi Takamasu

National Institute for Materials Science, 3-13 Sakura, Tsukuba 305-0003, Japan
(Received 6 November 2009; published 2 August 2010)

We report propagation of exciton polaritons (EPs) in photoexcited nanofibers of thiacyanine dye over a few hundred micrometers at room temperature. We determine the complex refractive index along the nanofibers by fluorescence microscopy measurements on single nanofibers and observe its anomalous behavior due to the EP effect. The longitudinal-transverse splitting energy (ΔE_{L-T}) is evaluated to be ~ 1 eV. The large ΔE_{L-T} and waveguide function of the nanofibers allow a millimeter propagation of EPs at room temperature, which is hardly realized in other systems.

Strong coupling between photons and excitons in the solid state results in the formation of exciton polaritons (EPs). EPs have attracted a great deal of interest because of their mixed characteristics of photons and excitons. In particular, the propagation of EPs in quasi-one-dimensional structures, e.g., nanofibers and nanowires, has been drawing much interest for both fundamental science and device applications. Because of the photon-exciton coupling, EPs show remarkable propagation properties in comparison with uncoupled light, such as anomalously low group velocity that leads to a substantially large refractive index of the media [1,2]. The large refractive index may enable nanofibers with subwavelength width to propagate the EPs and to steer them at wavelength scale. This opens up potential applications of nanofibers in EP-based optoelectronic circuits, which can be highly integrated compared to waveguide optical circuits.

To realize such nanofiber devices, EPs have to propagate over macroscopic distances, and hence, their stability is critical. The stability is governed by the exciton binding energy E_{ex} and the longitudinal-transverse exciton splitting energy $\Delta E_{L-T} = E_L - E_T = \hbar \omega_L - \hbar \omega_T$. Because of anticrossing between light and exciton dispersions, the dispersion curve of EP splits into the upper and lower EP branches [3]. ΔE_{L-T} represents the energy difference between the two branches and is related to the strength of the photon-exciton interaction. When E_{ex} and ΔE_{L-T} are greater than the thermal energy kT, the EPs can be stable and potentially propagate along the nanofibers. EP propagation in waveguides and quantum wells of inorganic semiconductors has been extensively studied [1,2]. Both E_{ex} and ΔE_{L-T} for these structures are at most 1 meV and much smaller than kT at room temperature ($kT_R = \sim 30$ meV) [4]. Thus, EP propagation can be observed only at cryogenic temperatures, preventing application to practical devices. Recent studies have shown that nanofibers of ZnO ($E_{ex} = \sim 60$ meV) show ΔE_{L-T} of up to ~ 160 meV, and formation of EP have been observed at room temperature [5]. The large ΔE_{L-T} is attributed to

both the large transition oscillator strength of ZnO and the effect of light confinement, which together enhance photon-exciton coupling. In this context, organic dye nanofibers offer the possibility of long-range EP propagation at room temperature owing to the condition E_{ex}, $\Delta E_{L-T} \gg kT_R$. Unlike Wannier excitons in inorganic semiconductors, Frenkel excitons in organic dye crystals have an E_{ex} of the order of eV. Moreover, organic dyes have a considerably larger oscillator strength compared to inorganic semiconductors. Nevertheless, fabrication techniques for high-quality organic nanofibers have not been well developed, while elaborate crystal growth and lithographical techniques are available for inorganic semiconductors. Since structural defects cause losses of EP, quality of nanofiber is important. In this respect, organic dyes were disadvantageous compared to inorganic semiconductors.

In this Letter, we report on fraction of a millimeter propagation of EPs in photoexcited organic dye nanofibers. Nanofibers of thiacyanine (TC) dye with lengths of ~ 250 μm act as "active" waveguides that propagate fluorescence (FL) over the entire length of the nanofibers [6]. We study the mechanism of the active waveguiding and demonstrate that FL propagates in the form of EPs. ΔE_{L-T} along nanofiber was evaluated to be ~ 1 eV. The large ΔE_{L-T} and a waveguide function of the nanofibers allow the long-range EP propagation at room temperature. Our results show that dye nanofibers are promising for EP-based nanofiber devices, and also that they may provide ideal systems to study the strong light-matter interactions.

TC (chemical formula in Refs. [6,7]) belongs to a class of cyanine dyes which are widely used as photosensitizers in the photographic industry. TC dissolved in water spontaneously forms defect-free nanofibers with lengths of up to ~ 250 μm [6,7]. Samples were prepared by drop-casting the solution onto a glass substrate (refractive index: 1.526) and allowing the solvent to evaporate. Atomic force microscopy observations show that the fibers have a rectangular cross section with typical heights and widths of 100–200 and 400–700 nm, respectively [6].

Figure 1(a) shows a FL microscopy image of a nanofiber recorded by exciting it with a focused laser beam (λ = 405 nm). FL spots were observed at both the fiber ends, showing that the fiber acts as an active waveguide. The waveguiding behavior is observed over ~250 μm without apparent loss [6,7]. Most of the nanofibers on the substrate are bent because of their highly flexible nature. Interestingly, efficient waveguiding was observed even along sharply bent nanofibers with a radius of curvature less than a few micrometers [6]. This indicates that the refractive index along the nanofiber is extraordinarily high for simple dielectric waveguides, suggesting that FL propagates as EPs. To prove the EP propagation, we determine the complex refractive index along the nanofibers $n_\parallel(\omega) + i\kappa_\parallel(\omega)$. The complex refractive index of macroscopic crystals is usually determined with the help of the Kramers-Kronig relation, which gives the relationship between $n(\omega)$ and $\kappa(\omega)$. To obtain accurate refractive index of the nanofibers, we determine them independently to each other by utilizing FL microscopy techniques.

$n_\parallel(\omega)$ was determined by observing the Fabry—Perot (FP) modes of single nanofibers. Since the nanofibers have well-defined end faces, they function as FP cavities. The approximate midpoint of a straight nanofiber was excited with a laser spot (λ = 405 nm, spot size: ~300 nm) and the FL was recorded using a charge-coupled device camera through an imaging monochromator. The recorded image is both spatially and spectrally resolved along two orthogonal axes. By positioning the nanofiber so that it is imaged between the entrance slits of the monochromator, the spectra at the fiber ends and at the excited position (i.e., the FL spectrum) can be extracted from the image [7]. Figure 1(b) shows the spectra at the end of nanofibers with lengths ranging from 3.6–18.6 μm. A series of peaks was observed over nearly the entire range of the spectra, and the spacing between the peaks decreased with fiber length. The spacing between FP modes is given by

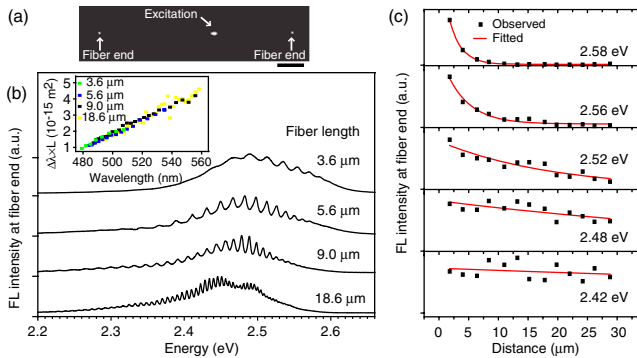$$\Delta\lambda = \lambda^2/2n_\parallel(\omega)L, \qquad (1)$$

where L is the cavity length. $\Delta\lambda \times L$ evaluated from the observed peak spacing and the fiber length is independent of the fiber length [the inset in Fig. 1(b)], proving that the peaks are due to FP modes. From the width of the peaks, the finesse of the cavities was determined to range from 0.7–3.0 depending on fibers and wavelengths. These values correspond to the end face reflectivity R_{end} of 0.06–0.20. From the observed $\Delta\lambda$, $n_\parallel(\omega)$ was evaluated using Eq. (1) [see Fig. 2(a)].

$\kappa_\parallel(\omega)$ was determined by measuring the decay of guided FL intensity as a function of guided distance. The spectra at one end of a 40-μm-long straight fiber were recorded by moving the laser spot along the fiber (step width: 500 nm). Each spectrum was normalized with respect to that at the excited position, because the intensity of light coupled into the nanofiber is proportional to that at the excited position. From the normalized spectra for different guided distances, which are expressed as $I(\omega, X = X')$ (X: guided distance), the decay curve of the guided light intensity at $\omega = \omega'$ was obtained in the form of $I(\omega = \omega', X)$. $I(\omega = \omega', X)$ for several ω' are shown in Fig. 1(c) (square dots). $I(\omega = \omega', X)$ is related to $\kappa_\parallel(\omega)$ through the following equation:

$$I(\omega = \omega', X) = I(\omega = \omega', X = 0)\exp[-2\omega'\kappa_\parallel(\omega')X/c], \qquad (2)$$

FIG. 1 (color online). (a) FL microscopy image of a TC nanofiber. Scale bar: 10 μm. (b) Spectra at the ends of nanofibers with different lengths. Inset: plots of $\Delta\lambda \times L$ against λ. (c) FL intensity at the end of a fiber versus the guided distance at different energies (square dots). Solid lines: best fitted curves.
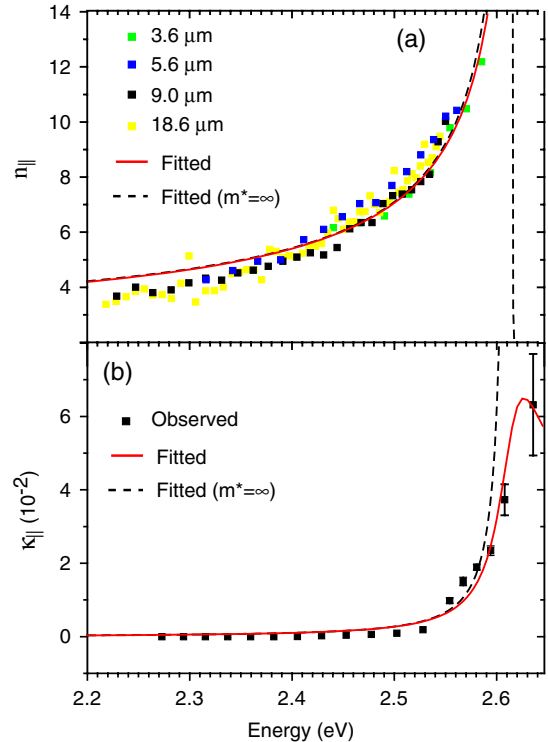

FIG. 2 (color online). (a) $n_\parallel(\omega)$ determined from the FP modes for fibers with different lengths (square dots). Best fitted curves obtained using the EP model with (solid line) and without (dashed line) the spatial dispersion effect of the exciton. (b) $\kappa_\parallel(\omega)$ determined by the decay of FL intensity (square dots). Best fitted curves obtained using the EP model with (solid line) and without (dashed line) the spatial dispersion effect.

where c is the speed of light [8]. $\kappa_{\parallel}(\omega')$ was determined by the best fit of Eq. (2) to the observed data [solid lines in Fig. 1(c)].

The experimentally determined $n_{\parallel}(\omega)$ and $\kappa_{\parallel}(\omega)$ are shown in Figs. 2(a) and 2(b) (square dots), respectively. The $n_{\parallel}(\omega)$ values obtained for nanofibers with different lengths show a single curve that dramatically increases with energy. $n_{\parallel}(\omega)$ exceeds 10 at energies close to 2.6 eV, which is an unusually large value for dielectric waveguides. This anomalous behavior of $n_{\parallel}(\omega)$ strongly suggests that guided FL propagates as EPs. $\kappa_{\parallel}(\omega)$ is nearly zero ($<5 \times 10^{-4}$) up to ~ 2.5 eV and starts to sharply increase at ~ 2.55 eV, implying that the attenuation of guided FL (EP) is very low below ~ 2.5 eV but rapidly increases above ~ 2.55 eV.

To obtain a further indication of the EP formation, we measured the reflection spectrum of the ensemble of nanofibers. In the EP model, incident light with energy between E_T and E_L is strongly reflected at the crystal surface due to the forbidden energy gap between them [3,4]. Thus, a broad reflection band with high reflectivity is characteristic of EP formation, and E_L (E_T) can be determined as the high- (low-) energy edges of the reflection band. Unpolarized light was focused onto the sample (spot size: ~ 300 μm) using an objective lens. Reflected light at the sample surface was analyzed using a spectrometer. There were about 50 randomly oriented nanofibers within the area of illumination. The spectrum shows a broad reflection band with a width of ~ 1 eV, providing further evidence of EP formation (Fig. 3) [9]. The reflection band has the sharp high-energy edge, and E_L was determined to be 3.64 eV from the energy at which the reflectivity drops to the minimum value. This value is confirmed by the EP model analysis presented next. The position of the low-energy edge could not be clearly determined, because a FL peak appeared in the energy region obscures it (Fig. 3). For macroscopic crystals with high reflectivity, the FL is far weaker than the reflection, but it is no longer negligible for narrow structures with widths $d \approx \lambda$.

We analyzed the measured $n_{\parallel}(\omega)$ and $\kappa_{\parallel}(\omega)$ within the EP model. This analysis allows us to determine the dispersion curves, the anticrossing behavior of which proves the EP formation. Because the fiber has a rectangular cross section with width of 400–700 nm ($\approx \lambda$) and height of 100–200 nm ($\ll \lambda$), the energy of light guided in the nanofiber is given by

$$\hbar \omega = \sqrt{\hbar^2 c^2 k_{\parallel}^2 + E_C^2}/[n_{\parallel}(\omega) + i\kappa_{\parallel}(\omega)], \quad (3)$$

where $k_{\parallel}$ is the wave vector parallel to the fiber and $E_C = \hbar c(\pi/d) = 1$ eV for $d = 600$ nm is the cutoff energy. Considering the far smaller Bohr radius of Frenkel excitons (<1 nm) compared to the nanofiber dimensions, we do not expect the effect of the finite dimensions on the excitons. Thus, we used the dielectric function derived from a simple Lorentz model, which is given by
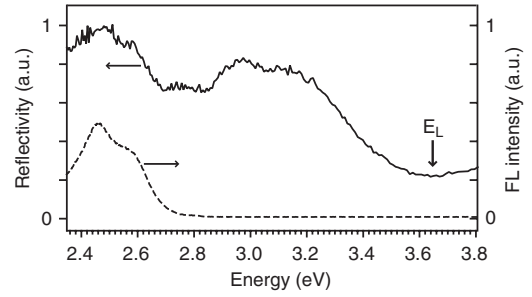

FIG. 3. Solid line: reflection spectrum of the ensemble of nanofibers. The FL spectrum (dashed line) shows that the peak in the reflection spectrum at ~ 2.5 eV is due to FL. E_L is determined at the reflection minimum (arrow).

$$\varepsilon(\omega, k_{\parallel}) = \varepsilon_b \left[1 + \frac{\omega_L^2 - \omega_T^2}{\omega_T^2 - \omega^2 + (\hbar k_{\parallel}^2 \omega_T/m*) - i\omega\gamma} \right]$$

$$= \frac{c^2 k^2}{\omega^2}, \quad (4)$$

where ε_b is the background dielectric constant, m^* is the exciton mass, and γ is the damping constant [3]. This provides the dispersion relation along the nanofiber. Equations for $n_{\parallel}(\omega)$ and $\kappa_{\parallel}(\omega)$ were obtained by eliminating $k_{\parallel}$ in Eq. (4) using Eq. (3) and were best fitted to the observed data using $E_L = 3.64$ eV and $E_C = 1$ eV. $E_T = 2.615$ eV, $\varepsilon_b = 4.22$, $\gamma = 2 \times 10^{-4}$ eV, and $m^* = 0.35 m_0$ (m_0: free electron mass) were obtained by the best fit, and the calculated $n_{\parallel}(\omega)$ and $\kappa_{\parallel}(\omega)$ of the lower EP branch well agree with the experimental data (solid lines in Fig. 2). We note that satisfactory fits could not be obtained when the spatial dispersion of the exciton was not taken into account (i.e., $m^* = \infty$): In this case, the calculated $\kappa_{\parallel}(\omega)$ curve diverges as the energy approaches E_T [dashed line in Fig. 2(b)], while the observed $\kappa_{\parallel}(\omega)$ curve is considerably flattened just below E_T. In Fig. 4, the dispersion curves for real $k_{\parallel}$ obtained by the analysis are shown with the FL spectrum. The anticrossing due to the EP effect and the forbidden energy gap between E_T and E_L are apparent, indicating that FL propagates as EPs. $\Delta E_{L-T} = E_L - E_T$ was obtained to be 1.02 eV.

By comparing ΔE_{L-T} of the nanofiber with that of a bulk TC crystal, one can examine the effect of light confinement on the photon-exciton coupling. Although ΔE_{L-T} of bulk TC has not been reported, probably due to difficulty in growing a macroscopic crystal, those of several other cyanine dyes with similar oscillator strengths to TC were determined by reflection spectroscopy. ΔE_{L-T} for these crystals was observed in the range 0.5–3 eV depending on molecules and crystal faces [10–12]. Then, ΔE_{L-T} of bulk TC is expected to be 0.5–3 eV. Since ΔE_{L-T} of 1.02 eV is within this range, it is safely deduced that the difference in ΔE_{L-T} between the nanofiber and the bulk TC is small, likely to be less than an order of magnitude. The small difference implies that the light confinement due to the FP effect has little influence on the photon-exciton coupling
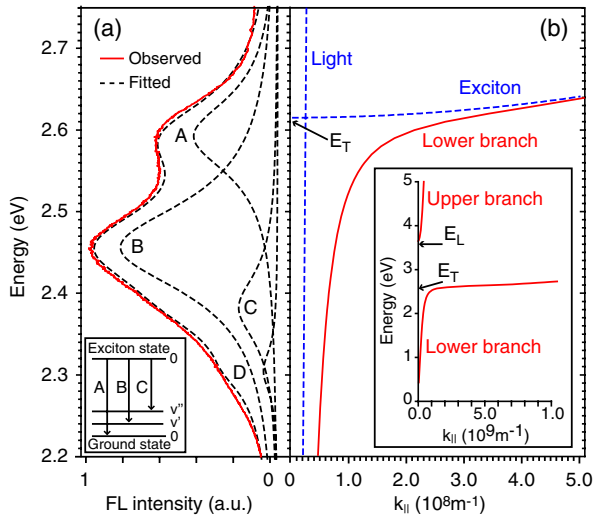
FIG. 4 (color online).   (a) FL spectrum of a nanofiber (solid line) and the best fitted curves (dashed lines). The fitted curves are slightly offset for visibility. Inset: schematic diagram of the transitions. (b) Solid line: dispersion curves of the lower branch EP. Dashed lines: dispersion curves of uncoupled light and exciton. Inset: wide view of the dispersion curves.

strength, as is expected from the low R_{end} values (0.06–0.20). This is further supported by the $n_{\parallel}(\omega)$ curves determined from different nanofibers [Fig. 2(a)]. They agree with each other although R_{end} is different for each nanofiber. This confirms that the FP effect practically does not influence the coupling strength, because the coupling modulates the $n_{\parallel}(\omega)$ curve. Consequently, EPs in TC nanofibers are characterized as bulk EPs formed by coupling between propagating FL and the excitons. Such bulk EPs can propagate independently of either the R_{end} value or fiber length, making the nanofibers promising for application in EP-based circuits.

The FL spectrum is composed of four Lorentzian peaks at 2.593 (A), 2.457 (B), 2.383 (C), and 2.305 eV (D) with homogeneous linewidths of ~0.1 eV [Fig. 4(a)]. We assigned the highest energy peak (A) to the transition from the exciton state to the ground state (the 0-0 transition) and the lower energy peaks (B–D) to vibronic transitions [the inset in Fig. 4(a)] on the basis of the assignment of solution spectra [13,14]. The dispersion curves show that these FL peaks are in the vicinity of the crossing point between the light and exciton dispersion curves, where the lower branch EPs dramatically change their character from excitonic to photonic with a decrease in energy [Fig. 4(b)]. FL in peak A forms the lower branch EPs with energies around E_T. These EPs have a large exciton character and their density of states is high. Thus, these EPs undergo fast nonradiative decay by scattering with acoustic phonons through their exciton character and rapidly attenuate. The large $\kappa_{\parallel}(\omega)$ in this energy region is attributed to the decay. On the other hand, FL in peaks B–D forms EPs with energies lower than E_T. Below E_T, the photon character dominates and the density of states is low, leading to the suppression of EP

decay, which is known as the bottleneck effect of EP [15]. This results in the small κ in this energy region, and these EPs propagate with low losses. Thus, the vibronic transitions play an essential role in the active waveguiding behavior.

It seems that the long-range EP propagation can occur in any other dye nanofibers when certain conditions are satisfied, such as the large oscillator strength of the molecules, a defect-free structure, and $d > \sim \lambda/2n_{\parallel}(\omega)$ to exhibit one propagation mode of light. Recently, the active waveguiding behaviors have been observed for a number of nanofibers of various classes of dyes [16]. Although they have been understood as simple optical waveguiding without considering the EP effect, the EP propagation may play a key role. Investigations on optical properties of these nanofibers from the view point of the EP model will lead to an elaborate understanding of the active waveguiding and will stimulate further studies toward their device applications.

*takazawa.ken@nims.go.jp
[1] R. G. Ulbrich and G. W. Fehrenbach, Phys. Rev. Lett. **43**, 963 (1979).
[2] S. Chu and S. Wong, Phys. Rev. Lett. **48**, 738 (1982).
[3] J. J. Hopfield, Phys. Rev. **112**, 1555 (1958).
[4] J. Lagois, Phys. Rev. B **23**, 5511 (1981).
[5] L. K. van Vugt et al., Phys. Rev. Lett. **97**, 147401 (2006); S. Rühle et al., Nano Lett. **8**, 119 (2008).
[6] K. Takazawa et al., Nano Lett. **5**, 1293 (2005); K. Takazawa, Chem. Phys. Lett. **452**, 168 (2008).
[7] K. Takazawa, J. Phys. Chem. C **111**, 8671 (2007).
[8] The influence of the reflection at the front and back end faces can be neglected because of the low R_{end} values.
[9] Note that the absolute reflectivity cannot be evaluated from ensemble spectrum. Nevertheless, the absolute reflectivity at 3.0 eV is 0.3–0.7, that was estimated from the reflection spectroscopy on single nanofibers. When light propagating along a fiber forms EPs, the reflectivity at the fiber end faces is nearly unity between E_T and E_L, while that at other faces is less than unity. Since our spectrum was measured at the side surfaces, the reflectivity less than unity is reasonable.
[10] H. J. Hesse et al., Phys. Status Solidi B **76**, 817 (1976).
[11] G. Weiser et al., Chem. Phys. **52**, 183 (1980).
[12] L. Dähne, Adv. Mater. **8** 486 (1996).
[13] C. Peyratout and L. Daehne, Phys. Chem. Chem. Phys. **4**, 3032 (2002).
[14] H. Mustroph et al., Chem. Phys. Chem. **10**, 835 (2009).
[15] Y. Toyozawa, Prog. Theor. Phys. Suppl. **12**, 111 (1959).
[16] Y. S. Zhao et al., Adv. Mater. **20**, 1661 (2008); Y. S. Zhao et al., Angew. Chem., Int. Ed. **47**, 7301 (2008); H. Wang et al., J. Mater. Chem. **19**, 89 (2009); F. Balzer et al., Appl. Phys. Lett. **82**, 10 (2003); F. Balzer et al., Phys. Rev. B **67**, 115408 (2003).